ChemComm

Accepted Manuscript

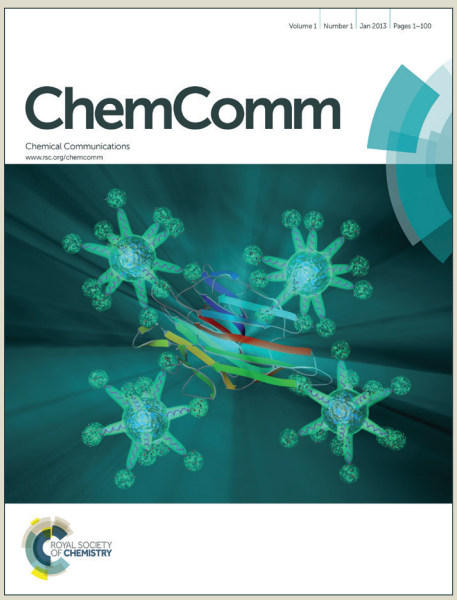

ROYAL SOCIETY OF CHEMISTRY

www.rsc.org/chemcomm

Colour graphic:

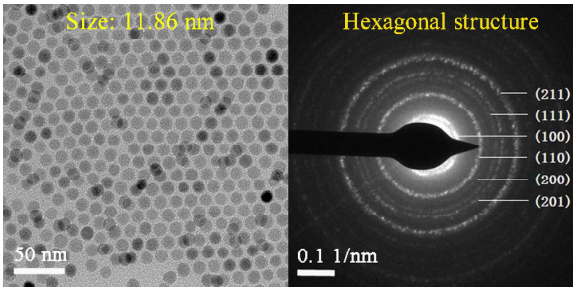

Text: Small-sized (~11.86 nm) hexagonal $NaYF_4$:Yb^{3+}, Er^{3+} nanocrystals have been synthesized by simultaneously controlling over the nucleation and growth process.

Journal Name

RSCPublishing

COMMUNICATION

Facile synthesis of small-sized and monodisperse hexagonal $NaYF_4:Yb^{3+}$, Er^{3+} nanocrystals

Cite this: DOI: 10.1039/x0xx00000x

Dongdong Li, Qiyue Shao,* Yan Dong and Jianqing Jiang

Received 00th January 2012,
Accepted 00th January 2012

DOI: 10.1039/x0xx00000x

www.rsc.org/

Small-sized (~11.86 nm) and monodisperse hexagonal $NaYF_4:Yb^{3+}$, Er^{3+} upconversion (UC) nanocrystals have been successfully synthesized by simultaneously controlling over the nucleation and growth process with a relatively high oleic acid to precursors ratio.

Photoluminescence (PL) materials that have unusual and excellent optical properties have shown great potential as sensitive bioprobes for biomedical applications.[1,2] Among various PL materials, lanthanide-doped upconversion nanoparticles (UCNPs), which are capable of converting long wavelength near-infrared (NIR) radiation into a visible or NIR emission through an upconversion process, have received great research interest.[3-5] Compared with the traditionally used down conversion fluorescent organic dyes and quantum dots, UCNPs exhibit higher signal-to-noise ratios, lower photodamage and deeper penetration depth in tissue, making them ideal for use as luminescent probes in biological labelling and imaging technology.[6, 7]

Hexagonal phase (β-) $NaYF_4:Yb^{3+}$, Er^{3+} have been demonstrated to be the most efficient upconversion materials. However, most of the uniform β-$NaYF_4:Yb^{3+}$, Er^{3+} reported recently are >20 nm in size,[8-10] which are not optimal for their use as bioprobes. Considering the body clearance of nanoparticles and imaging sensitivity, the nanocrystals with strong upconversion luminescence (UCL) and relative small particle size are of fundamental requirement for their biomedical applications. However, it is still a great challenge to synthesize small and monodisperse hexagonal $NaYF_4:Yb^{3+}$, Er^{3+} nanocrystals with bright UC emission. Prasad et al have reported the monodisperse and ultrasmall cubic $NaYF_4:Yb^{3+}$, Tm^{3+} nanocrystals with sizes of 7-10 nm.[11] However, the cubic phase only offers about an order-of-magnitude lower of upconversion efficiency relative to its hexagonal phase counterpart. In the presence of oleylamine as surfactant, Cohen et al and Yi et al have synthesized ultrasmall hexagonal $NaYF_4:Yb^{3+}$, Er^{3+} nanocrystals with diameter about 4.5 and 11.1 nm, respectively.[12,13] Unfortunately, a few cubic phase impurities still existed in their final products. Recently, the doping of lanthanide ions with a size larger than Y^{3+} ions (like Gd^{3+}) was found to facilitate the synthesis of hexagonal structure, and ultrasmall (sub-10 nm) β-$NaYF_4:Yb^{3+}$, Er^{3+} nanocrystals have been prepared by Gd^{3+} ions doping at different levels.[14-16] However, the synthesis of pure hexagonal $NaYF_4:Yb^{3+}$, Er^{3+} nanocrystals with a relative small particle size is still a great challenge until now.

It is well known that hexagonal phase $NaYF_4$ is thermodynamically more stable than cubic phase, thus an energy barrier must be overcome for the phase transition from cubic to hexagonal.[17] However, this process is complicated and difficult to control due to several stages including the consumption of cubic phase and the nucleation and growth of hexagonal phase are highly overlapped. Therefore, the ability to improve the nucleation rate of hexagonal phase and simultaneously slow its growth rate is critical for the synthesis of small-sized β-$NaYF_4:Yb^{3+}$, Er^{3+} nanocrystals. Herein, we present a facile method to synthesize small-sized hexagonal $NaYF_4:Yb^{3+}$, Er^{3+} nanocrystals using oleic acid (OA) as the only capping ligand. The nucleation and growth process of hexagonal phase can be effectively controlled with a relatively high OA to precursor ratio, which may be suggestive for the synthesis of other types of nanocrystals, especially for those exist in diverse crystal structures.

In a typical synthetic route, 0.3 mmol rare-earth (RE) acetates (Y/Yb/Er=78:20:2) with 20 ml of OA and 100 ml of 1-octadecene (ODE) were added to a flask under vigorous stirring. The solution was heated to 100 ℃ to remove oxygen and residual water. After cooling to 50 ℃, a methanol solution (10 ml) containing NH_4F (1.2 mmol) and NaOH (0.75 mmol) was added, and the resulting solution was kept at 50 ℃ for 30 min. After methanol was evaporated, the solution was heated to 300 ℃ under an argon atmosphere for 90 min. The nanoparticles were precipitated by the addition of ethanol and isolated via centrifugation.

The transmission electron microscope (TEM) images of the as-prepared $NaYF_4:Yb^{3+}$, Er^{3+} nanocrystals are shown in Fig. 1 (a) and (b). It can be seen that these nanocrystals are monodispersed and spherical in shape. The average diameter was determined to be 11.86 ± 0.78 nm by random measurements of more than 200 particles. High-resolution TEM (HRTEM) image reveals that the UCNPs are of single-crystalline nature (Fig. 1c). The selected-area electron diffraction (SAED) pattern (Fig. 1d) shows spotty polycrystalline diffraction rings corresponding to the (100), (110), (111), (200), (201), and (211) planes of the hexagonal $NaYF_4$ lattice. The hexagonal phase structure is further identified by the HRTEM image. The lattice distance is 0.35 nm, corresponding to the *d*-spacing for the (0001) lattice plane of the hexagonal $NaYF_4$ structure (Fig. 1c).

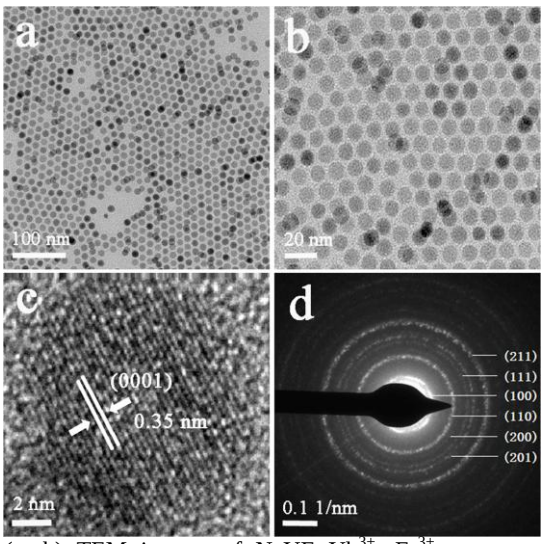

Fig.1 (a, b) TEM images of $NaYF_4$:Yb^{3+}, Er^{3+} nanocrystals at different magnifications, (c) HRTEM image of a single $NaYF_4$:Yb^{3+}, Er^{3+} nanocrystals, and (d) SAED pattern of $NaYF_4$:Yb^{3+}, Er^{3+} nanocrystals.

To understand the possible mechanism, we performed a series of experiments to investigate the role of OA and ODE on the synthesis of $NaYF_4$:Yb^{3+}, Er^{3+} nanocrystals. As shown in Fig. 2 (a), uniform β-$NaYF_4$:Yb^{3+}, Er^{3+} nanocrystals with the average diameter of 22.56 nm were obtained when 6 ml of OA and 15 ml of ODE were used. As the content of ODE increased to 30 ml (Fig. 2 b), the particle size does not present noticeable difference, and the crystalline structure also keeps unchanged. This indicates that 1-octadecene, as the non-coordination solvent, contributes little to the size control of UCNPs, and has no direct relation with the phase transition from cubic to hexagonal. Fig. 2 (c) shows the TEM image of $NaYF_4$:Yb^{3+}, Er^{3+} nanocrystals synthesized in pure ODE. It can be seen that only big and agglomerated nanoparticles were obtained. This suggests that

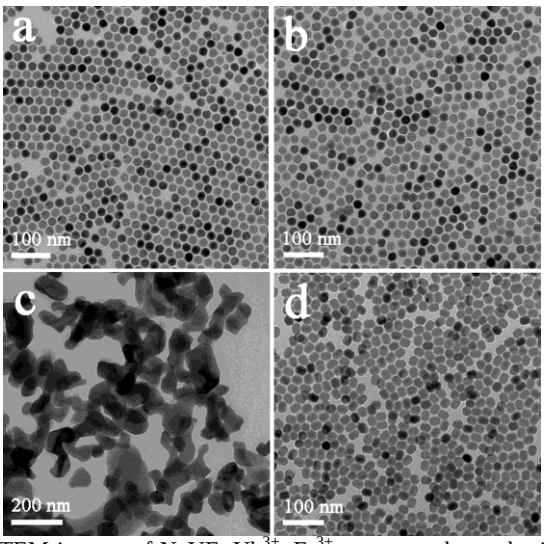

Fig.2 TEM images of $NaYF_4$:Yb^{3+}, Er^{3+} nanocrystals synthesized at various contents of OA/ODE: (a) 6 ml/15 ml, (b) 6 ml/30 ml, (c) 0 ml/21 ml, and (d) 12 ml/30 ml. Other synthesis conditions: 1 mmol of RE acetates, 2.5 mmol of NaOH, 4 mmol of NH_4F, 300 ℃ for 90 min.

the presence of OA is the premise for the synthesis of $NaYF_4$:Yb^{3+}, Er^{3+} nanocrystals with desirable size and structure. To further understand the role of OA, the precursor concentration was reduced by increasing the contents of OA and ODE to 12 and 30 ml, respectively (Fig. 2 d). Comparing the experimental result in Fig. 2 (a), an obvious shape evolution from sphere to rod can be observed and the particle size increases to 31.65 × 24.68 nm. The shape evolution can be attributed to the preferential adsorption of excess OA onto the $(10\bar{1}0)$ planes, which leads to the rapid growth along the *c*-axis.[8,18] However, due to the little contribution of ODE on particle size (Fig. 2 b), it is reasonable to believe that the increased particle size in Fig. 2 (d) was also induced by OA, since the amount of OA is the only parameter that was changed. In addition, Fig. 2 (d) also shows that the small-sized β-$NaYF_4$:Yb^{3+}, Er^{3+} nanocrystals cannot be synthesized by only reducing the concentration of precursors.

These experimental results suggest that OA instead of ODE plays the key role in controlling the size and structure of $NaYF_4$:Yb^{3+}, Er^{3+} nanocrystals. When the reaction was performed in pure ODE, due to the low solubility of rare-earth acetates and NaF, the nucleation process mainly occurred on their interfaces. The low crystallization speed and insolubility of UCNPs in ODE result in the big and agglomerated nanoparticles. However, when oleic acid was added, the crystallization speed and monomer concentration were both improved due to the high solubility of NaF, F^- and $RE(oleate)_3$ in oleic acid.[19] As a result, the nucleation and growth processes of UCNPs were accelerated in the presence of OA.

According to the above analysis, we believe that a higher content of OA would further increase the nucleation rate of UCNPs, which is benefit for the synthesis of β-$NaYF_4$:Yb^{3+}, Er^{3+} nanocrystals with a smaller size. However, this approach also results in a higher monomer concentration, and thus a higher growth rate of UCNPs (see Fig. 2 d). To restrain the growth process of existing nuclei, we explored a relatively high oleic acid to precursor ratio (20 ml of OA to 0.3 mmol of rare-earth acetates). Through this adjustment, the nucleation rate of UCNPs was enhanced, and simultaneously the growth of existing nuclei was effectively retarded owing to the dilution of monomers. As a result, the β-$NaYF_4$:Yb^{3+}, Er^{3+} nanocrystals with a small size were obtained (Fig. 1). It should be noted that the morphology of UCNPs is sensitive to the ratios of OA to ODE.[18] Therefore, 100 ml of ODE was adopted for the synthesis of 11.86 nm β-$NaYF_4$:Yb^{3+}, Er^{3+} nanocrystals to avoid the resulting morphology evolution.

To confirm this mechanism, Fig. 3 (a) shows the $NaYF_4$:Yb^{3+}, Er^{3+} nanocrystals synthesized in 9 ml of OA and 12 ml of ODE. Compared with the spherical nanoparticles in Fig. 2 (a), the rod-shaped nanoparticles with a bigger particle size were obtained, which is consistent with the observation in Fig. 2 (d). Although the crystallization speed was improved with the increase of OA, the higher monomer concentration resulted in an enhanced growth rate of $NaYF_4$:Yb^{3+}, Er^{3+} nanocrystals. Fig.3 (b) shows the UCNPs synthesized in 10 ml of OA and 100 ml of ODE using 0.3 mmol of RE acetates as precursor. Unlike the experimental result in Fig. 1, β-$NaYF_4$:Yb^{3+}, Er^{3+} nanocrystals with a bigger size (17.72 ± 0.88 nm) were obtained. Due to the less amount of OA, the crystallization speed was reduced. Moreover, the high monomer concentration led to the high growth rate of UCNPs. As the content of OA increased to 30 ml, β-$NaYF_4$:Yb^{3+}, Er^{3+} nanocrystals with the average diameter of 13.85 ± 1.26 nm were prepared (Fig. 3 c). Compared with the observation in Fig. 1, the slight increase in particle size relates to the anisotropic growth of UCNPs can be attributed to the higher OA/ODE ratio.

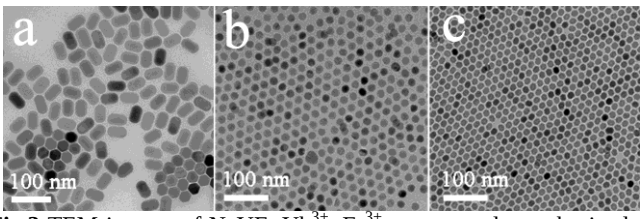

Fig.3 TEM images of $NaYF_4$:Yb^{3+}, Er^{3+} nanocrystals synthesized at different conditions: (a) 1 mmol of RE acetates in 9 ml/12 ml of OA/ODE, 0.3 mmol of RE acetates in (b) 10 ml/100 ml of OA/ODE and (c) 30 ml/100 ml of OA/ODE. Other synthesis conditions: 300 ℃ for 90 min.

Fig. 4 shows the corresponding UCL spectra of the cubic and hexagonal $NaYF_4$:Yb^{3+}, Er^{3+} nanocrystals. Under 980 nm laser excitation, green and red upconversion emissions centered at around 525, 545, and 660 nm were observed, corresponding to the $^2H_{11/2}\rightarrow{}^4I_{15/2}$, $^4S_{3/2}\rightarrow{}^4I_{15/2}$, and $^4F_{9/2}\rightarrow{}^4I_{15/2}$ transitions of Er^{3+} ions, respectively. Compared with the cubic $NaYF_4$:Yb^{3+}, Er^{3+} nanocrystals in a similar particle size, an obvious UCL enhancement can be observed for hexagonal $NaYF_4$:Yb^{3+}, Er^{3+} UCNPs. In addition, it can be found that the green to red emission intensity ratio (GRR) of β-$NaYF_4$:Yb^{3+}, Er^{3+} nanocrystals is significantly higher than that of cubic $NaYF_4$:Yb^{3+}, Er^{3+} UCNPs. Due to the similar particle size and identical surface adsorbed ligands, the improved GRR of β-$NaYF_4$:Yb^{3+}, Er^{3+} nanocrystals can be attributed to the fewer lattice defects. It implies that the synthesized β-$NaYF_4$:Yb^{3+}, Er^{3+} nanocrystals possess a high crystallinity and thus an excellent UCL efficiency.

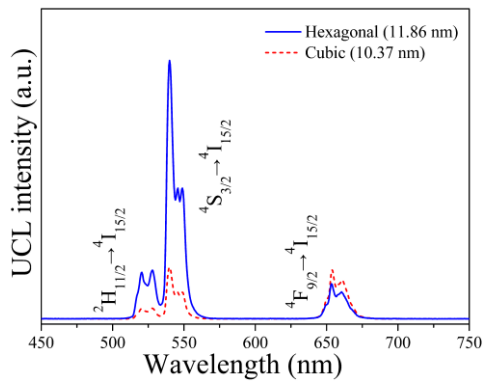

Fig.4 UCL spectra of cubic and hexagonal $NaYF_4$:Yb^{3+}, Er^{3+} nanocrystals with similar particle size.

In summary, we presented a facile method for the synthesis of small-sized hexagonal $NaYF_4$:Yb^{3+}, Er^{3+} nanocrystals. It was found that 1-octadecene contributes little to the size and phase control of $NaYF_4$:Yb^{3+}, Er^{3+} nanocrystals. However, the nucleation and growth processes of UCNPs can be effectively controlled with a relatively high oleic acid to precursor ratio. When 20 ml of OA and 0.3 mmol of rare-earth acetates were used, the nucleation rate of β-$NaYF_4$:Yb^{3+}, Er^{3+} nanocrystals was enhanced, and simultaneously the growth of existing nuclei was retarded owing to the low monomer concentration. We believe that this approach provides a novel route to control the particle size of UCNPs, and may be suggestive for the synthesis of other types of nanocrystals, especially for those exist in diverse crystal structures.

The work was financially supported by the Natural Science Foundation of China (NSFC) (No. 51302038), the Natural Science Foundation of Jiangsu Province of China (Nos. BK2011064 and BK2012346). The work was also supported by the Fundamental Research Funds for the Central Universities (No. CXLX12_0083) and the Scientific Research Foundation of Graduate School of Southeast University (No. YBJJ1351).

Notes and references

Jiangsu Key Laboratory of Advanced Metallic Materials, Department of Materials Science and Engineering, Southeast University, Nanjing 211189, People's Republic of China.
E-mail: qiyueshao@seu.edu.cn

Electronic Supplementary Information (ESI) available: Detailed synthesis procedures and characterization. See DOI: 10.1039/c000000x/

1 G. E. LeCroy, S. K. Sonkar, F. Yang, L. M. Veca, P. Wang, K. N. Tackett, J. J. Yu, E. Vasile, H. J. Qian, Y. M. Liu, P. J. Luo and Y. P. Sun, *ACS Nano*, 2014, **8**, 4522-4529.
2 C. Li, *Nat. Mater*., 2014, **13**, 110-115.
3 L. L Liang, Y. M. Liu and X. Z. Zhao, *Chem. Commun*., 2013, **49**, 3958-3960.
4 A. Podhorodecki, M. Banski, A. Noculak, B. Sojka, G. Pawlik and J. Misiewicz, *Nanoscale*, 2013, **5**, 429-436.
5 Q. B. Xiao, Y. T. Ji, Z. H. Xiao, Y. Zhang, H. Z. Lin and Q. B. Wang, *Chem. Commun*., 2013, **49**, 1527-1529.
6 Z. Y. Hou, C. X. Li, P. A. Ma, Z. Y. Cheng, X. J. Li, X. Zhang, Y. L. Dai, D. M. Yang, H. Z. Lian, and J. Lin, *Adv. Funct. Mater*., 2012, **22**, 2713-2722.
7 X. M. Liu, M. Zheng, X. G. Kong, Y. L. Zhang, Q. H. Zeng, Z. C. Sun, W. J. Buma and H. Zhang, *Chem. Commun*., 2013, **49**, 3224-3226.
8 Z. Q. Li and Y. Zhang, *Nanotechnology*, 2008, **19**, 345606.
9 J. C. Boyer, C. J. Carling, B. D. Gates and N. R. Branda, *J. Am. Chem. Soc*., 2010, **132**, 15766-15772.
10 Q. Wang, Y. X. Liu, B. C. Liu, Z. L. Chai, G. R. Xu, S. L. Yu and J. Zhang, *CrystEngComm*, 2013, **15**, 8262-8272.
11 G. Y. Chen, T. Y. Ohulchanskyy, R. Kumar, H. Ågren and P. N. Prasad, *ACS Nano*, 2010, **4**, 3163-3168.
12 A. D. Ostrowski, E. M. Chan, D. J. Gargas, E. M. Katz, G. Han, P. J. Schuck, D. J. Milliron and B. E. Cohen, *ACS Nano*, 2012, **6**, 2686-2692.
13 G. S. Yi and G. M. Chow, *Adv. Funct. Mater*., 2006, **16**, 2324-2329.
14 F. Wang, Y. Han, C. S. Lim, Y. H. Lu, J. Wang, J. Xu, H. Y. Chen, C. Zhang, M. H. Hong and X. G. Liu, *Nature*, 2010, **463**, 1061-1065.
15 F. Shi and Y. Zhao, *J. Mater. Chem. C*, 2014, **2**, 2198-2203.
16 N. J. J. Johnson, W. Oakden, G. J. Stanisz, R. S. Prosser and F. C. J. M. van Veggel, *Chem. Mater*., 2011, **23**, 3714-3722.
17 Y. Q. Sui, K. Tao, Q. Tian, and K. Sun, *J. Phys. Chem. C*, 2012, **116**, 1732-1739.
18 H. Na, K. Woo, K. Lim and H. S. Jang, *Nanoscale*, 2013, **5**, 4242-4251.
19 C. H. Liu, H. Wang, X. Li and D. P. Chen, *J. Mater. Chem.*, 2009, **19**, 3546-3553.